IEEE Photonics Journal
An IEEE Photonics Society Publication

Open Access

Ultra-Small and Fabrication-Tolerant Silicon Polarization Beam Splitter Using Sharp Bent Directional Coupler

Volume 10, Number 5, September 2018

Xiaodong Wang
Xueling Quan
Wei Zhang
Jie Hu
Chong Shen
Xiulan Cheng

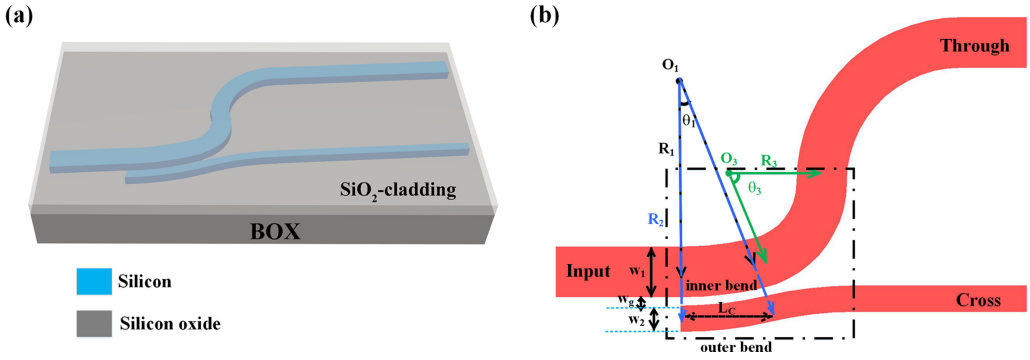

DOI: 10.1109/JPHOT.2018.2873629
1943-0655 © 2018 IEEE

IEEE photonics SOCIETY

IEEE

Ultra-Small and Fabrication-Tolerant Silicon Polarization Beam Splitter Using Sharp Bent Directional Coupler

Xiaodong Wang,[1,2] **Xueling Quan**,[1] **Wei Zhang**,[1,2] **Jie Hu**,[1,3] **Chong Shen**,[1,2] **and Xiulan Cheng**[1]

[1]Center for Advanced Electronic Materials and Devices, Shanghai Jiao Tong University, Shanghai 200240, China
[2]Department of Micro-nanoelectronics, Shanghai Jiao Tong University, Shanghai 200240, China
[3]Department of Electronic Engineering, Shanghai Jiao Tong University, Shanghai 200240, China

DOI:10.1109/JPHOT.2018.2873629

Manuscript received August 10, 2018; revised September 27, 2018; accepted September 28, 2018. Date of publication October 4, 2018; date of current version October 16, 2018. This work was supported by the Ministry of Science and Technology of the People's Republic of China under Grant 2016YFB0200205.
Corresponding author: Xiulan Cheng (e-mail: xlcheng@sjtu.edu.cn).

Abstract: An ultra-small polarization beam splitter on silicon-on-insulator platform is proposed and demonstrated experimentally employing a sharp bent directional coupler. The coupling length of our device is only 0.764 μm. High-efficient selective coupling can be achieved benefiting from the inner bend chosen as Through port and ultra-small bend (radii are about 3 μm) used in Through and Cross waveguides. The measured excess loss is less than 1 dB and extinction ratio is 15–20 dB for TM polarization, meanwhile, the measured excess loss is less than 2 dB and extinction ratio is 15-16 dB for TE polarization in a wavelength range from 1540 nm to 1580 nm. The fabrication tolerance to variation of waveguide width is also demonstrated. When the waveguide widths of the Through and Cross waveguides vary from -24 nm to $+12$ nm, the measured excess losses remain lower than 2 dB and the extinction ratios are higher than 10 dB for both polarizations. The footprint of the fabricated device is just 1.5 μm $\times$ 1.3 μm.

Index Terms: Waveguides, waveguide devices.

1. Introduction

The high refractive index contrast between silicon and silicon oxide cladding results in serious birefringence, which leads to polarization sensitivity [1]–[3]. Polarization beam splitter (PBS) plays a critical role in polarization handling devices for separating or combining two orthogonal polarizations [4]. Various kinds of structures have been proposed for realizing PBSs, including directional couplers (DCs) [5]–[8], grating assisted contra-directional couplers [9], [10], asymmetrical Mach-Zehnder interferometers (MZIs) [11], [12], out of plane grating [13], multimode interferences (MMIs) [14]–[16], photonic crystals (PhCs) [17], [18] and so on.

Compactness is a key requirement for photonic integrated circuit to realize high density integration [19], [20]. A great deal of devices has been demonstrated with ultra-small footprints [21], [23]. An ultra-compact silicon topology-photonic PBS using inverse design was reported with a footprint of

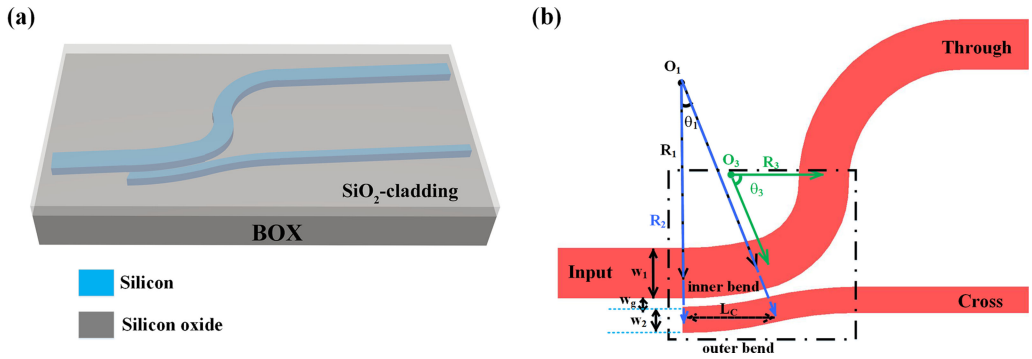

Fig. 1. Schematic structure of the proposed ultra-small bent DC PBS, (a) the 3D view, (b) the plan view.

2.4 μm $\times$ 2.4 μm [24]. However, a small feature size was required in its fabrication. Benefiting from the weak optical confinement in a sharp bent waveguide and strong coupling between bent DC waveguides, bent DCs can be used to realize compact devices [25]. A silicon PBS using a bent DC based on phase matching condition was reported with a footprint of 9.5 μm $\times$ 2.8 μm [26]. We have fabricated a bent DC PBS with a more compact footprint by introducing sharp bends and shown preliminary results [27].

In this paper, we propose and demonstrate an ultra-small bent DC PBS. The radii of $\sim$3 μm for bends are adopted in Cross and Through ports to reduce the footprint. Considering that the TM polarization leaks more easily from inner bend to outer bend than TE polarization, the inner bend is chosen as Through port. Therefore, the coupling length and the footprint can be reduced, which is different from the design in ref. [26]. For TM polarization, the highly efficient selective coupling between two bends can be achieved over a coupling length of 0.764 μm, which is attributed to good phase matching for TM mode in two bends and the inner bend chosen as Through waveguide. A small bend (radius is 0.72 μm) connected to Through waveguide is used to filter out the residual TM-polarized light. And the width of Cross waveguide is chosen close to the cutoff width for TE mode. As a result, the polarization extinction ratios (PERs) over 15 dB for both polarizations are achieved. Large tolerance to waveguide width for fabricated PBS is also demonstrated. The upper-cladding of the PBS is SiO_2. The device achieves a record small footprint of 1.5 μm $\times$ 1.3 μm, to the best of our knowledge.

2. Device Design and Fabrication

Figs. 1(a) and (b) show schematic structure of the proposed bent DC PBS. There are two parallel sharp bends with radii of about 3 μm in two ports. The loss introduced by sharp bends can be alleviated by advanced fabrication processes and reducing the propagation length [28]. Ultra-low loss 0.086 $\pm$ 0.005 dB per 90° bend with TE polarization input for bending radius of 1μm are demonstrated without any special fabrication process [29]. In our design, the inner bend is chosen as Through port because of the easier coupling from inner to outer bend for TM-polarized light, which is different from the design in ref. [26]. The TM polarization satisfies the phase matching condition in Through and Cross waveguides, meanwhile, the difference value of optical path length (OPL) in two ports for TE polarization should be large enough. For the TM polarization, strong cross-coupling is achieved from Through port to Cross port, and then outputs by Cross port. The sharp bend ($R_3 = 0.72$ μm) in the Through port is used to filter out the residual TM-polarized light and increase the PER. For the TE polarization, the light goes directly at Through port without coupling. The width of Cross waveguide is approximate to the cutoff width of TE mode ($\sim$220 nm) [30], as a result, the PER can be improved significantly. The bent waveguides connected to the coupling region at two ports are used to separate the Through and Cross waveguides.

A silicon-on-insulator (SOI) wafer with 220 nm thick top silicon and 3 μm thick buried oxide is adopted in our bent DC PBS. The design parameters are labeled in Fig. 1(b). The inner bend with

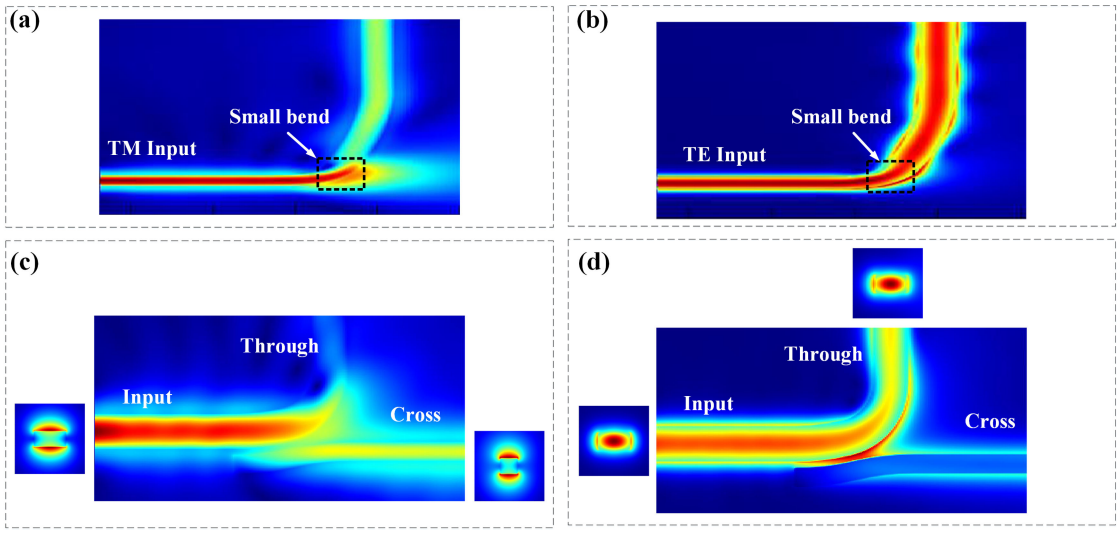

Fig. 2. The Simulated electric field distribution in small bend (R_3) at 1550 nm for the (a) TM-polarized light input; (b) TE-polarized input. The Simulated electric field distribution in proposed bent DC PBS at 1550 nm for the (c) TM polarization; (d) TE polarization.

radius (R_1) of 3 μm is set as Through port. The widths of Through and Cross bent waveguides are chosen according to the phase matching condition:

$$\mathrm{OPL} = n_1 k_0 R_1 \theta_1 = n_2 k_0 R_2 \theta_1 \qquad [26]$$

in which n_1 and n_2 are the effective refractive indices of the TM mode in the Through and Cross waveguides, respectively; k_0 is the wavenumber in vacuum; R_1 and R_2 are the radii of Through and Cross waveguides, and θ_1 is the angle of coupling region. There should be a large phase-mismatch in two bends for TE polarization. The gap between two bends (w_g) is set as w_g. The radius of Cross waveguide is given by $R_2 = R_1 + w_1/2 + w_g + w_2/2$. The finite difference eigenmode (FDE) solver is applied to calculate the OPLs for both polarizations. In order to achieve the aforementioned condition, different parameters have been swept including the angle of coupling region (θ_1), w_g and the widths of two bends (w_1, w_2). When θ_1, w_g, w_1, and w_2 are 13°, 80 nm, 438 nm, and 226 nm, respectively, the difference value of OPL in two bends for TM polarization is only 0.05. The TE polarization cannot be supported by Cross port, whereas the TE polarization can be confined well in Through port, which insure the significant difference value of OPL in two ports. The radius (R_3) and the angle (θ_3) of the bend in the Through port are 0.72 μm and 77° to filter out the residual TM-polarized light. The electric fields distribution at 1550 nm for this small bend connected with another large bend ($R = 10$ μm, $\theta = 13°$) are shown in Figs. 2(a) and (b), which are simulated by three-dimensional finite-difference time-domain (3D-FDTD) method. For TM-polarized light input, there is only 45% of input left with serious leakage, whereas, for the TE-polarized light input, 91% of input can go through the small bend with slight radiation. Thus the small bend (R_3) can improve the performance of the PBS without introducing into larger excess loss. The coupling length for bent DC can be calculated by $L_c = R_2 \sin\theta_1 = 0.764$ μm. the footprint of our device is 1.5 μm $\times$ 1.3 μm labeled by a black dashed frame in Fig. 1(b).

Figs. 2(c) and (d) show the light propagation for the proposed PBS simulated by 3D-FDTD method at 1550 nm with different polarizations. The insets at different ports show the electric fields distribution at cross section. In condition of the TM-polarized light input, strong coupling occurs between two bends and most light outputs at Cross port. As we can see, the small bend R_3 acts as a filter for residual TM polarization. Whereas the TE-polarized light can go directly along the Through port.

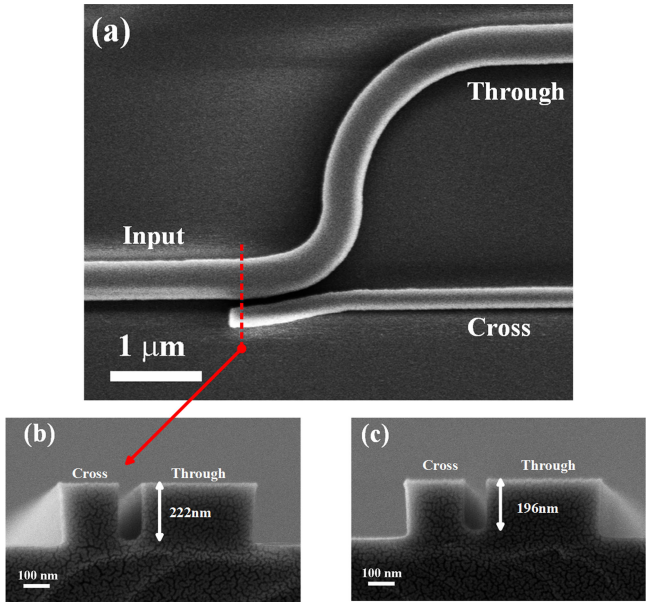

Fig. 3. (a) FESEM image of a fabricated PBS. (b-c) Cross-sections of the gap between the Through and Cross waveguides in this work and our previous work [27], respectively. Gold nanoparticles with several nanometers thick are deposited on the cross-sections to obtain clear SEM images.

For the fabrication of proposed PBS, the full-etched waveguides pattern was defined by electron-beam lithography (EBL, Vistec EBPG 5200), and then transferred by inductively coupled plasma (ICP) dry etch. Thereafter, shallow etched (70 nm) grating couplers were made by EBL via ICP dry etch. Finally, silicon oxide was deposited by plasma enhanced chemical vapor deposition (PECVD) for protection. The field emission scanning electron microscope (FESEM) image of the fabricated PBS without upper cladding is shown in Fig. 3(a). The width of gap (w_g) is the feature size in the PBS, which is 80 nm. We find that the gap is difficult to be fully etched as shown in Fig. 3(c), which would degrade the performance. Compared with our previous work [27], we increase the ICP etch time to ensure the fully etched gap in fabrication, as shown in Fig. 3(b). In this way, better performances are achieved. Note that the Cross and Through waveguides are slightly over-etched. In the measurements, a tunable laser (Keysight 81960A) was used as the source. An optical power meter (Keysight 81636B) was used to detect the transmission spectra at both output ports. The polarization of input was determined by the type of polarization-dependent grating couplers. In order to characterize the performance of our device, two identical proposed PBS were fabricated closely with different grating couplers on the same chip. At the central wavelength of $\lambda = 1550$ nm, the transmission for the TM- and TE- polarized grating couplers are -5.9 dB/port and -5.4 dB/port, respectively.

3. Result and Discussion

Fig. 4 shows the measured results. The transmission spectra of fabricated PBS were normalized by the transmission of straight waveguide connected with grating couplers. It can be seen that in the wavelength range of 1540-1580 nm, attribute to high efficient cross-coupling between Through and Cross waveguides and the filter effect by small bend (R_3), the excess loss and PER for TM polarization are below 1 dB and over 15 dB, respectively. In the wavelength range of 1515–1580 nm, for both polarizations, the excess losses can keep below 2.5 dB and PERs can keep over 10 dB. For TE polarization, high-power optical signal is obtained at the Through port. The excess loss and PER are lower than 2 dB and more than 15 dB, respectively. The high PER for TE polarization can

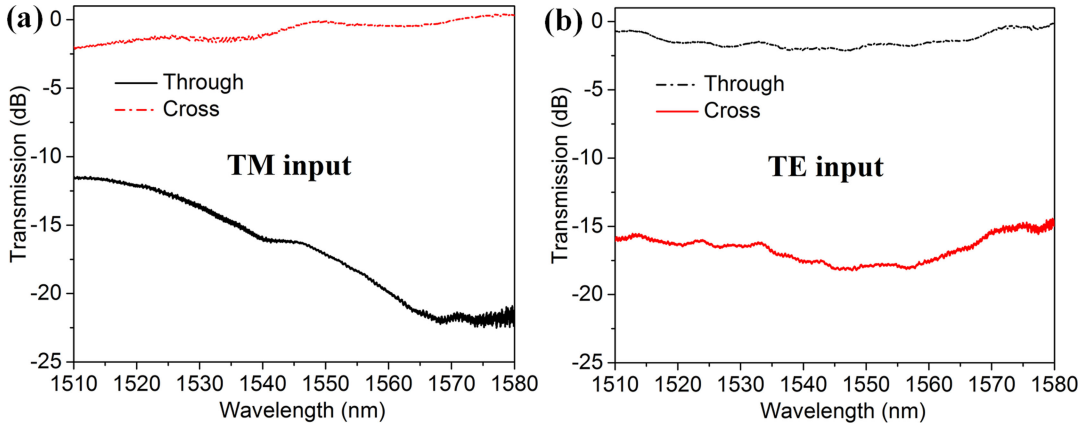

Fig. 4. Measured transmission spectra for the fabricated PBSs (a) TM-polarization light input; (b) TE-polarization light input.

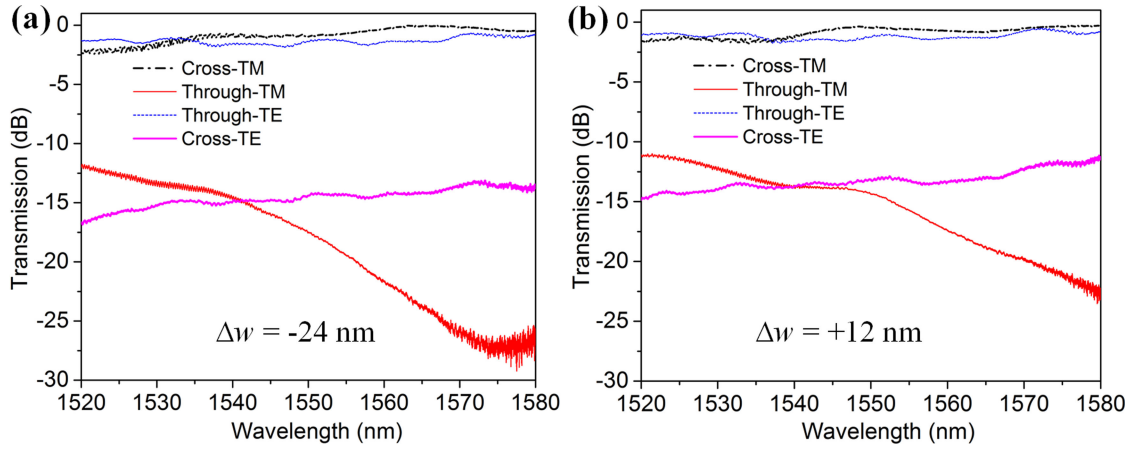

Fig. 5. Measured transmission spectra at the Through and Cross ports with different polarizations for the PBSs with width variations of (a) Δw $= -24$ nm and (b) Δw $= +12$ nm.

be attributed to the different cutoff widths for both modes. The TE mode will be cutoff, when the width of waveguide is below 220 nm, whereas the TM mode can propagate well [30]. The cascade or filter structures can be used to improve the PERs for both modes further [31], [32].

The fabrication tolerance to waveguide width of our PBS is also presented. The PBSs with different width variations for both Through and Cross waveguides were fabricated on the same chip. The widths of Through and Cross port were varied with the same step 6 nm. When the waveguide variations change from Δw $= -24$ nm to Δw $= +12$ nm, the PERs for both polarization can remain higher than 10 dB. Figs. 5(a) and (b) show the measured transmission spectra of Δw $= -24$ and $+12$ nm, respectively. For TM polarization, the excess losses for Cross port increase about 1 dB due to the mismatch of OPL caused by width variation. While for TE polarization, the excess losses for Through port keep in the same level. In wavelength range of 1540 nm to 1580 nm, the excess losses for both polarizations are below 2 dB for the width variations Δw $= -24$ nm and $+12$ nm. The PERs for both polarizations are higher than 12 dB and 10 dB for Δw $= -24$ nm and $+12$ nm, respectively. In wavelength range of 1525-1580 nm, for both polarizations and width variations, the excess losses can keep lower than 2.5 dB and PERs can keep higher than 10 dB. The results show that the demonstrated PBS is tolerant to width variations.

TABLE 1
Performances of Other Different Silicon Polarization Beam Splitters

Structure	Footprint (μm × μm)	PERs (dB)	Excess loss (dB)	Operation bandwidth （nm）	Tolerance
DC [5]	7 × 16	~ 15	< 0.5	40	20 nm for width 40 nm for gap
Grating-assisted contradirectional coupler [10]	~ 30 × 2	30	< 1	21	±10 nm for width
MZI [12]	173.8 × 3.36	> 10	< 2.5	40	NA
MMI [16]	202 × 6	> 12	< 2	50	NA
Topology-photonic structure [24]	2.4 × 2.4	> 10	< 1.5	32	±20 nm for thickness
Bent DC [26]	9.5 × 2.8	> 10	< 1	200	±60 nm for width
This work	1.5 × 1.3	> 15	< 2	40	-24 nm to +12 nm for width

We compare the proposed ultra-small PBS with other different PBSs in the literature, as shown in Table 1. Our proposed PBS achieves the smallest footprint and is tolerant to waveguides width variations.

4. Summary

In conclusion, we have proposed and experimentally demonstrated an ultra-compact PBS employing a sharp bent directional coupler. The coupling length and footprint of the PBS are 0.764 μm and 1.5 μm $\times$ 1.3 μm, respectively. The PERs and excess losses are over 15 dB and below 2 dB in a wavelength range from 1540 nm to 1580 nm for both TE and TM polarizations, respectively. It has been shown that the fabricated PBSs are tolerant to width variation. When the widths of Through and Cross ports vary from $-$24 nm to $+$12 nm, the excess losses are lower than 2 dB, and over 10 dB for PERs can be guaranteed.

References

[1] C. Manolatou and H. A. Haus, “High density integrated optics,” in *Passive Components for Dense Optical Integration*. New York, NY, USA: Springer, 2002, pp. 97–125.
[2] D. Dai, L. Liu, S. Gao, D. X. Xu, and S. He, “Polarization management for silicon photonic integrated circuits,” *Laser Photon. Rev.*, vol. 7, pp. 303–328, 2013.
[3] Y. Zhang *et al.*, “Ultra-compact and highly efficient silicon polarization splitter and rotator,” *APL Photon.*, vol. 1, 2016, Art. no. 091304.
[4] Y. Zhang *et al.*, “On-chip silicon polarization and mode handling devices,” *Frontiers Optoelectron.*, vol. 11, pp. 77–91, 2018.
[5] H. Fukuda, K. Yamada, T. Tsuchizawa, T. Watanabe, H. Shinojima, and S.-I. Itabashi, “Ultrasmall polarization splitter based on silicon wire waveguides,” *Opt. Exp.*, vol. 14, pp. 12401–12408, 2006.

[6] M.-A. Komatsu, K. Saitoh, and M. Koshiba, "Design of miniaturized silicon wire and slot waveguide polarization splitter based on a resonant tunneling," *Opt. Exp.*, vol. 17, pp. 19225–19234, 2009.
[7] Y. Yue, L. Zhang, J. Y. Yang, R. G. Beausoleil, and A. E. Willner, "Silicon-on-insulator polarization splitter using two horizontally slotted waveguides," *Opt. Lett.*, vol. 35, pp. 1364–1366, 2010.
[8] S. Lin, J. Hu, and K. B. Crozier, "Ultracompact, broadband slot waveguide polarization splitter," *Appl. Phys. Lett.*, vol. 98, 2011, Art. no. 151101.
[9] H. Qiu, Y. Su, P. Yu, T. Hu, J. Yang, and X. Jiang, "Compact polarization splitter based on silicon grating-assisted couplers," *Opt. Lett.*, vol. 40, pp. 1885–7, May 1, 2015.
[10] Y. Zhang *et al.*, "High-extinction-ratio silicon polarization beam splitter with tolerance to waveguide width and coupling length variations," *Opt. Exp.*, vol. 24, pp. 6586–6593, 2016.
[11] W. N. Ye, D. X. Xu, S. Janz, and P. Waldron, "Stress-induced SOI Polarization Splitter Based on Mach–Zehnder Interferometers (MZI)," in *Proc. Int. Conf. Group IV Photon.*, 2006, pp. 249–251.
[12] D. Dai, Z. Wang, J. Peters, and J. E. Bowers, "Compact polarization beam splitter using an asymmetrical Mach–Zehnder interferometer based on silicon-on-insulator waveguides," *IEEE Photon. Technol. Lett.*, vol. 24, no. 8, pp. 673–675, Apr. 2012.
[13] J. Feng and Z. Zhou, "Polarization beam splitter using a binary blazed grating coupler," *Opt. Lett.*, vol. 32, pp. 1662–1664, 2007.
[14] Y. Ding, H. Ou, and C. Peucheret, "Wideband polarization splitter and rotator with large fabrication tolerance and simple fabrication process," *Opt. Lett.*, vol. 38, pp. 1227–1229, 2013.
[15] Y. Huang, Z. Tu, H. Yi, Y. Li, X. Wang, and W. Hu, "High extinction ratio polarization beam splitter with multimode interference coupler on SOI," *Opt. Commun.*, vol. 307, pp. 46–49, 2013.
[16] W. Yang, Y. Xu, Y. Li, X. Wang, and Z. Wang, "A compact and wide-band polarization beam splitter based on wedge-shaped MMI coupler in silicon-on-insulator," in *Proc. Int. Conf. Opt. Fiber Commun. Conf. Exhib.*, 2015, Paper W2A. 12.
[17] X. Ao, L. Liu, L. Wosinski, and S. He, "Polarization beam splitter based on a two-dimensional photonic crystal of pillar type," *Appl. Phys. Lett.*, vol. 89, pp. 171115-1–171115-3, 2006.
[18] P. Rani, Y. Kalra, and R. K. Sinha, "Complete photonic bandgap-based polarization splitter on silicon-on-insulator platform," *J. Nanophoton.*, vol. 10, 2016, Art. no. 026023.
[19] P. P. Absil *et al.*, "Silicon photonics integrated circuits: A manufacturing platform for high density, low power optical I/O's," *Opt. Exp.*, vol. 23, pp. 9369–9378, Apr. 6, 2015.
[20] P. Dong *et al.*, "224-Gb/s PDM-16-QAM modulator and receiver based on silicon photonic integrated circuits," in *Proc. Opt. Fiber Commun. Conf. Expo. Nat. Fiber Opt. Eng. Conf.*, 2013, pp. 1–3.
[21] W. M. Green, M. J. Rooks, L. Sekaric, and Y. A. Vlasov, "Ultra-compact, low RF power, 10 Gb/s silicon Mach-Zehnder modulator," *Opt. Exp.*, vol. 15, pp. 17106–17113, 2007.
[22] W. Yang, M. Yin, Y. Li, X. Wang, and Z. Wang, "Ultra-compact optical 90° hybrid based on a wedge-shaped $2\times$ 4 MMI coupler and a $2\times$ 2 MMI coupler in silicon-on-insulator," *Opt. Exp.*, vol. 21, pp. 28423–28431, 2013.
[23] L. Gao, Y. Huo, J. S. Harris, and Z. Zhou, "Ultra-compact and low-loss polarization rotator based on asymmetric hybrid plasmonic waveguide," *IEEE Photon. Technol. Lett.*, vol. 25, no. 21, pp. 2081–2084, Nov. 2013.
[24] B. Shen, P. Wang, R. Polson, and R. Menon, "An integrated-nanophotonics polarization beamsplitter with 2.4 $\times$ 2.4 μm2 footprint," *Nat. Photon.*, vol. 9, pp. 378–382, 2015.
[25] H. Morino, T. Maruyama, and K. Iiyama, "Reduction of wavelength dependence of coupling characteristics using Si optical waveguide curved directional coupler," *J. Lightw. Technol.*, vol. 32, no. 12, pp. 2188–2192, Jun. 2014.
[26] D. Dai and J. E. Bowers, "Novel ultra-short and ultra-broadband polarization beam splitter based on a bent directional coupler," *Opt. Exp.*, vol. 19, pp. 18614–20, 2011.
[27] Y. Zhang *et al.*, "Ultra-compact silicon polarization beam splitter with a short coupling length of 0.768 μm," in *Proc. Int. Conf. Opt. Fiber Commun.*, 2018, Paper Th2A. 10.
[28] Q. Xu, D. Fattal, and R. G. Beausoleil, "Silicon microring resonators with 1.5-μm radius," *Opt. Exp.*, vol. 16, pp. 4309–4315, 2008.
[29] Y. A. Vlasov and S. J. McNab, "Losses in single-mode silicon-on-insulator strip waveguides and bends," *Opt. Exp.*, vol. 12, pp. 1622–1631, 2004.
[30] Y. Xu and J. Xiao, "Compact and high extinction ratio polarization beam splitter using subwavelength grating couplers," *Opt. Lett.*, vol. 41, pp. 773–6, Feb. 15, 2016.
[31] S. Chen, H. Wu, and D. Dai, "High extinction-ratio compact polarisation beam splitter on silicon," *Electron. Lett.*, vol. 52, no. 12, pp. 1043–1045, Jun. 2016.
[32] H. Wu and D. Dai, "High-performance polarizing beam splitters based on cascaded bent directional couplers," *IEEE Photon. Technol. Lett.*, vol. 29, no. 5, pp. 474–477, Mar. 2017.